

Eigenshape Analysis of Planetary Craterforms: Implications for the Formation of Paterae on Io. T. J. Slezak¹, J. Radebaugh¹, and E.H. Christiansen¹, ¹College of Physical and Mathematical Sciences, Department of Geological Sciences, Brigham Young University, Provo, UT 84602, (tjs@byu.edu).

Introduction: The shapes of craterforms, circular to sub-angular depressions of no implied origin, are genetically related to the physical processes from which they originate. Paterae, inferred volcanic collapse features on Io, are highly irregular craterforms with scalloped edges [1] that constitute ~2.5% of Io's global surface area [2]. The complex shapes of paterae and the processes which form them are little understood. Though they bear some similarities, paterae are not directly analogous to any structures with well understood formation mechanisms, such as volcanic calderas, pit craters, or impact craters. This study analyzes two-dimensional shape to examine similarities in craterforms in order to determine if feature classification can be related to differences in formation mechanisms. In doing so, this study examines the variables that contribute to different morphologies. Distinctions in shape among known craterform populations can be used to strengthen inferences of the processes involved in the formation of paterae. A more thorough understanding of the differences in shape that are connected to the formation processes of craterforms will enhance our knowledge of the geologic history of planetary surfaces.

Background: Geological shape-classification systems [3], such as the Powers (1953) sphericity-roundness scale, demonstrate that the variations in shape of geological forms are powerful metrics to infer processes of origin and evolution [4]. A similar shape classification system may be used to infer the formation processes of craterforms by comparing variations in the mean shapes among end-members of distinct processes. Differences in outline shapes can be quantified and used as a metric for morphological interpretations of landforms.

While many other morphometric studies have used scalar aspects derived from shape, such as depth to diameter ratios or best-fit ellipses (e.g., [5] and [6]) to portray feature geometry, this study uses the scale-invariant shape information preserved in the outline of the feature. This is useful because paterae on Io are insufficiently described by traditional metrics due to deficiencies in the global Io dataset and the unique geometry of patera shapes.

Methods: We employ the methods of geometric morphometrics - the quantitative representation and analysis of morphology using geometric coordinates of outline shape instead of scalar measurements [7]. These methods are commonly used by paleontologists to ex-

amine fossil shapes and by biologists to examine evolutionary divergence in the morphology of organisms such as ostracods and fish.

The shapes of paterae on Io are compared with calderas on Mars, terrestrial ash-flow calderas and basaltic shield volcanoes, and lunar impact craters. We used the criteria of Pike and Clow (1981) as modified by Radebaugh (1999) to classify the groups of volcanoes examined in this study [8-9]. Locations for terrestrial basaltic shield volcanoes and ash-flow calderas are sourced from global databases [10-12] with supplementary records for ash-flow volcanoes [13-14]. Observations of martian calderas are reported by prior studies [15-18]. Lunar impact crater classifications are sourced from Wilhelms (1987) and the Lunar and Planetary Institute's Lunar Impact Crater Database [19-20]. Each craterform observation is outlined from imagery using a stereographic (conformal) map projection and a scaling factor is retained separately for each observation.

Applications of Eigenshape Analysis: Figure 1 illustrates the differences in impact crater morphology across the simple-complex crater transition on the Moon [19] using Eigenshape analysis [21-22]. The first step in

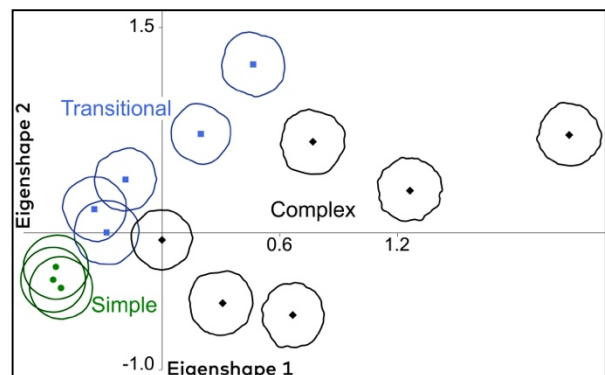


Figure 1. *Principal component analysis of geometric shapes for simple, transitional, and complex lunar impact craters provides a scale-invariant graphical depiction of the lunar simple-complex crater transition using shape alone.*

the procedure is to digitize the craterform outline by placing points along the bounds of an imaged craterform using the tpsDig software [23]. Next, the outline is interpolated to 100 equidistantly-spaced points and then transformed from Cartesian coordinates into quantitative measures of shape using the Zahn and Roskies (1972), or Z-R, shape function [24]. The Z-R shape function determines the *net angular deviation from a circle* by computing the angles between the interpolated

points of each outline. These measures are scale-invariant and isolate shape as a variable that can be quantitatively compared. After the shape function results are computed, the major correlations and relative differences in craterform shape are examined by plotting the results using principal components analysis.

By comparing the first two computed principal components of shape (eigenshapes), the lunar simple to complex transition is depicted in the plot using scale invariant measures. The first Eigenshape, the Eigenshape-1 (y -axis) represents the correlation of each shape to the approximate average of all of the shapes compared in the analysis. The second Eigenshape, the Eigenshape-2 (x -axis) represents the principal dimension of shape variation about that average between the groups. The outline of each crater is over plotted onto its corresponding data point. Simple craters plot similarly and have lesser variance, while transitional and complex craters plot farther away and have greater variance. Figure 1 shows that scale-dependent morphogenetic relationships can be expressed using scale-invariant measures of shape.

Results: Initial results from outline-based shape analysis of various types of craters are shown in Figure 2. Confidence interval ($\alpha=.05$) ellipses are displayed to

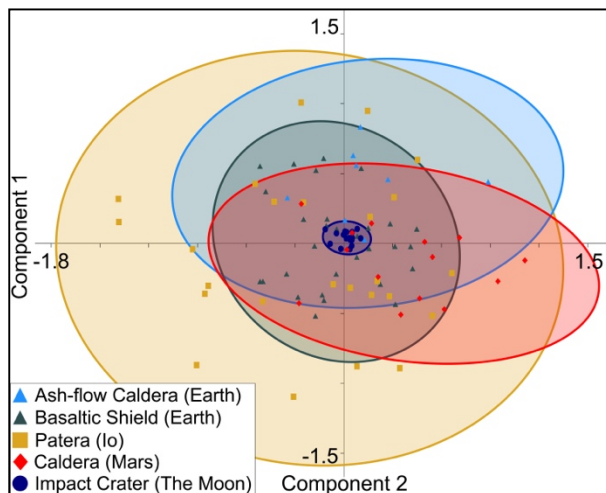


Figure 2. Eigenshape analysis of paterae on Io, calderas on Mars, terrestrial ash-flow calderas and basaltic shields, and lunar impact craters.

examine major trends and variance among the groups and provide a range of 95% confidence that the mean of the population falls within the ellipse. For the sample of paterae examined in the analysis, 15 lie within the 95% confidence interval for ash-flow calderas, 14 for basaltic shield volcanoes, and 13 for martian calderas. The same impact craters displayed in Figure 1 plot in a tight cluster and are easily differentiated from the other structures in comparison. Paterae show the greatest variance in shape among all of the craterform populations. The plot

shows identifiable trends among similar craters and differences in the variation between each group of craters. This plot supports the descriptive criteria used for qualitative and scale-based classification used to identify various craterforms.

Conclusion: Eigenshape analysis is an effective way to quantify and compare crater morphology. Io's paterae have unique shapes, but are most similar to terrestrial ash-flow calderas in their shapes. The scope of inference for the initial results of the study are limited by the variance in the number of samples included for each craterform population, and no casual inferences can be stated. If the shapes of volcanic craterforms and mechanisms of formation can be genetically linked using quantitative classifications, new insights in the formation process of paterae on Io may be revealed. The study will continue to refine and test its inferences as additional data of planetary surfaces are collected.

Future Work: More shape data for each type of craterform will be collected to enhance the comparative analysis. Inclusion of craters formed by other processes (e.g., karst or pit craters) should improve our ability to infer the processes of patera formation. Constructing a geological shape classification system for craterforms from end-member forms could greatly increase our understanding of craterform diversity and the processes involved in patera formation.

References: [1] Radebaugh J. et al. (2001) *JGR*, 106, 33005-20. [2] Williams D. A. et al. (2011) *GSA Sp. Pap.*, 483, 449-464. [3] MacLeod N. (2002) *Earth Sci. Rev.*, 59, 27-47. [4] Powers M. C. (1953) *J. Sed. Petr.*, 23, 117-119. [5] Zuber M. T. and Parmentier E. M. (1984) *Icarus*, 60, 200-210. [6] Pike R. J. and Davis P. (1984) *LPSC XV*, 645. [7] Rohlff F.J. and Marcus, L.F. (1993) *Trends Eco. Evo.*, 8, 129-132. [8] Pike R. J. and Clow, G. D. (1981) *USGS, OFR 81-1038*. [9] Radebaugh J. and Christiansen E. H. (1999) *LPSC XXX*, 1466. [10] Pieri D. C. et al. (2007) *AGU Fall Meeting*, #IN33A-0806. [11] Venzke E. (2013) *Global Volcanism Program*, Smithsonian Institution. [12] Geyer A. and Marti J. (2008) *J. Volc. Geotherm. Res.*, 175, 334-354. [13] Lipman P. (1997) *Bull. Volc.*, 59, 198-218. [14] Hughes G. R. and Mahood G. A. (2008) *Geo.*, 36, 8, 627-630. [15] Hodges C. A. and Moore H. J. (1994) *USGS Pro. Pap.*, 1534. [16] Robbins S. J. et al. (2011) *Icarus*, 211, 1179-1203. [17] Tanaka K. L. et al. (2014) *USGS, SIM 3292*. [18] Williams D. A. et al. (2009) *Plan. Spa. Sci.*, 57, 895-916. [19] Wilhelms D. (1987) *USGS, OFR 1348*. [20] Losiak A. et al. (2009) *LPI Lunar Exploration Intern Program*. [21] Lohmann G. P. (1983) *Math. Geo.*, 15, 6, 659-672. [22] MacLeod N. (1999). *Paleobio.* 25(1), 107-138. [23] Rohlff F.J. (2002) *tps Software Series*. [24] Zahn C. T. and Roskies R. Z. (1972) *IEEE Tran., Comp.*, C-21, 269-281.